Polish J. Chem., **78**, 803–814 (2004) **ORGANIC CHEMISTRY**

Selective Formation of Isopropyl α- and β-Glucofuranosides in One Pot Reaction from D-Glucose and Propanol-2 Promoted by V_2O_5

by S.K. Tyrlik[1*], E. Bednarek[2,5], W. Bocian[2], J. Sitkowski[2,3], J. Maurin[2,4], M. Olejnik[3], B. Nalewajko[1] and L. Kozerski[2,3*]

[1]*Department of Chemistry, University of Podlasie, 08-110 Siedlce, ul. 3-go Maja 54, Poland*
[2]*National Institute of Public Health, 00-725 Warszawa, ul. Chełmska 30/34, Poland*
[3]*Institute of Organic Chemistry, Polish Academy of Sciences, 01-224 Warszawa, ul. Kasprzaka 44, Poland*
[4]*Institute of Atomic Energy, 05-400 Otwock-Świerk, Poland*
[5]*Industrial Chemistry Research Institute, 01-793 Warszawa, ul. Rydygiera 8, Poland*

(Received January 28th, 2004; revised manuscript February 24th, 2004)

Reaction of D-glucose with propanol-2 promoted by V_2O_5 gives rise exclusively to isopropylglucofuranosides. Their tetraacetates were prepared; X-ray structure of one of tetraacetates was determined. ^1H and ^{13}C NMR signals assignment was done by COSY and GMBC techniques. Mechanism of selective glucosidation was discussed.

Key words: D-glucose, glucofuranosides, vanadium pentoxide, NMR, X-ray structure

There exist many reasons for a search for novel methods of synthesis of alkylglycosides, having carbohydrates and alcohols as substrates: the necessity to avoid formation of oligomeric species, to avoid protection and deprotection steps, formation of mixtures of pyranosides and furanosides *etc*. Alkylglycosides have biodegradable properties [1], so their presence in detergents and cosmetics is obviously advantageous [2].

Several papers appeared recently on application of sulphonated resins [3], acid zeolites [4] and clays [5] as heterogeneous catalysts of glycosidation, where mixtures of furanosides and pyranosides were obtained.

We became interested, whether simple binary oxides would promote synthesis of glycosides and what will be the selectivity of such process. We tried the following oxides in attempted reaction of D-glucose with ethanol: ZnO, SnO, PbO, CoO, CuO, Cr_2O_3, Fe_2O_3, Fe_3O_4, FeO, CdO, MnO, NiO, Al_2O_3, V_2O_5 and TiO_2 but no glycosides were formed. However, we observed in reaction of D-glucose with propanol-2, that vanadium and titanium oxides promote formation of glucosides, which could be either pyranosides or furanosides. Preliminary GC/MS analysis indicated presence of only two products.

*Corresponding author. Tel.: 6323221 ext 2018; Fax: 6326681; e-mail lkoz@icho.edu.pl

As simple NMR identification of alkyl glucofuranosides can be rather equivocal [3a], we decided to use thoroughly the modern multiple 2D NMR techniques and to perform X-ray structural determinations in order to gain conclusive assignments of NMR signals and to asses selectivity unambiguously. As products observed with vanadia and titania were formed in yield 3–7.5%, we searched for modification of vanadia until the better yields were obtained.

EXPERIMENTAL

Reaction and isolation of products: Oxides and D-glucose were commercial products used without any purification (oxides were used as polycrystalline powders without any pretreatment).

A typical reaction: 10.42 mmol of an oxide and 8.33 mmol of D-glucose were refluxed in 20 mL of *i*-PrOH with agitation for 24 hours. In the case of PbO and CuO, propanol solutions became slightly yellow, but in other cases reaction mixtures remained colourless. Propanol-2 was evaporated and residue was Soxhlet extracted with ethyl ether. Only for vanadium and titanium oxides evaporation of ether afforded an organic residue, which supposed to be a mixture of glucosides. Capillary gas chromatogram of crude reaction mixture is shown in Fig. 1.

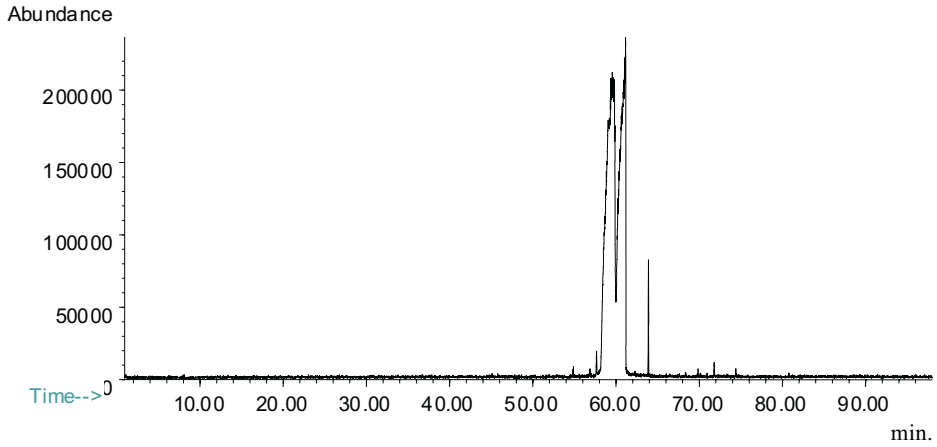

Figure 1. Capillary gas chromatogram of crude reaction mixture.

Yields of the crude products, obtained with vanadium oxide and with titanium oxide, were 7.5% and 3.0%, respectively. Increasing the reaction time to 48 h, only slightly improved the yield. 0.114 g of a products mixture was chromatographed on 5 g of silica gel 230–400 mesh; with 4% MeOH in $CHCl_3$ to give compound (**1**) (0.04 g) and (**2**) (0.05 g) as oils.

Mass spectral data: Compound (**1**). Mw 222; m/z (rel. intensity): 161(9), 131(3), 119(22), 116(6), 114(3), 103(5), 102(4), 101(9), 91(9), 89(12), 87(17), 86(10), 85(21), 74(6), 63(100), 72(10), 71(14), 70(11), 69(13), 61(32), 60(16), 57(13), 56(5), 55(3), 47(3), 45(13), 44(9), 43(36), 42(4), 41(16), 39(4). Compound (**2**). Mw 222; m/z (rel. intensity): 161(10), 131(4), 119(23), 116(5), 115(3), 103(5), 102(10), 101(15), 98(4), 97(3), 91(9), 89(9), 87(14), 86(5), 83(3), 74(6), 73(100), 72(7), 71(16), 70(8), 69(11), 61(34), 60(16), 57(12), 65(6), 55(3), 47(3), 45(15), 44(9), 43(35),42(4), 41(16), 39(4).

The molecular weights of compounds (**1**) and (**2**) were confirmed using LSIMS technique: For (**1**) m/z = 223 $(M+H)^+$; 245 $(M+Na)^+$; 445 $(2M+H)^+$; 467 $(2M+Na)^+$. For (**2**) m/z = 223 $(M+H)^+$; 245 $(M+Na)^+$; 267 $(M-H+Na)^+$ ions were recorded.

Specific rotations: for (**1**) $[\alpha]_D$ +121°; for (**2**) $[\alpha]_D$ –110°.

Modifications of vanadium oxide: To get better yields, following reactants were used to modify vanadium oxide: acids (HCl, HI, CF_3COOH, H_2SO_4), selected transition metal chlorides, bromides and iodides ($FeCl_3 \cdot 6H_2O$, $RuCl_3 \cdot H_2O$, $RhCl_3 \cdot H_2O$, $RhBr_3 \cdot H_2O$, $RhI_3 \cdot H_2O$, CuCl, CuBr), selected low valency transition metal complexes ($[PPh_3]_3RhCl$, $[PPh_3]_2Rh(CO)Cl$, $[PPh_3]_2cpRuCl$, cp_2TiCl_2, where Ph and cp stands for phenyl and cyclopentadienyl, respectively). 0.26–1.05 mmoles of vanadium oxide was suspended in 10–30 mL of solvent (methanol, ethanol, propanol-2, ethyl ether, THF, methyl formate, ethyl acetate) and 0.01–0.18 mmoles of reactant was added.

Two series of experiments were performed: at room temperature and in the reflux. Precipitate was filtered, dried at room temperature and used in a catalytic reaction as described above. The highest yield of the catalytic reaction (13%) was obtained with vanadium oxide modified with hydrated rhodium iodide (molar ratio vanadium oxide/rhodium iodide = 100) in methanol (rhodium iodide concentration 5.6×10^{-4} m/l), room temperature during 24 hours.

Acetylation of (1) and (2): To 0.07 g of compound (**1**) or (**2**) 1 mL of pyridine, 1.3 mL of acetic anhydride and a crystal of DMAP were added. After 24 hours the mixture was diluted with water and extracted with CH_2Cl_2. Extract was washed subsequently with diluted HCl, water solution of sodium bicarbonate and water. Crude product was chromatographed on silica gel (1.5 g; 230–400 mesh) and eluted with 5% acetone in hexane to give acetylation products (**3**) or (**4**). Compound (**3**) was crystallized from acetone/hexane; m.p. 77–78°C.

Mass spectral data: Compound (**3**). Mw 390; m/z (rel. intensity): 331(9), 256(3),245(29), 243(6), 242(12), 229(3), 210(3), 203(5), 200(16), 199(8), 186(3), 185(10), 182(5), 171(3), 170(4), 169(33), 168(8), 161(3), 158(9), 157(28),145(25), 144(7), 143(70), 141(12), 140(25), 139(5), 131(3), 129(3), 128(9), 127(14), 126(6), 116(3), 115(26), 113(12), 112(34), 109(12), 103(25), 102(4), 101(13), 99(7), 98(34), 97(13), 89(6), 86(7), 86(3), 86(11), 84(5), 81(18), 73(13), 71(3), 70(11), 69(13), 61(5), 60(3), 57(3), 44(3), 43(100), 41(6). Compound (**4**). Mw 390; m/z (rel. intensity): 331(4), 245(7), 242(5), 216(3), 200(6), 169(11), 158(3), 157(14), 145(9), 143(17), 141(4) ,140(9), 128(4), 127(5), 115(15), 113(14), 112(15), 109(4), 103(12), 101(4), 98(15), 97(6), 89(3), 36(4), 85(5), 81(9), 73(8), 70(6), 69(7), 43(100).

The molecular weights of compounds (**3**) and (**4**) were confirmed using LSIMS technique: For (**3**) m/z = 413 $(M+Na)^+$; measurement of atomic composition for this ion indicates $C_{17}H_{26}O_{10}Na$. For (**4**) m/z = 391 $(M+H)^+$; 413 $(M+Na)^+$.

Specific rotations: for (**3**) $[\alpha]_D$ +147°; for (**4**) $[\alpha]_D$ –34°.

Measurements of MS spectra: Low resolution EI mass spectra were recorded on a Hewlett-Packard 5972 mass selective detector coupled to a HP 5890 Series II gas chromatograph. The electron energy was 70 eV and the ion source temperature 170°C. We were using HP 5-MS capillary column. Temperature program: 35°C/30 min; 5°C/min. up to 250°C; 250°C 5 min.

Attempted identification of chromatographic peaks, using the Wiley Library with PBM search algorithm indicated a mass spectrum unknown to the library. For LSIMS technique a AMD-604 double focussing mass spectrometer (AMGD Intectra GmbH, Harpsted, Germany) equipped with a 10 keV cesium gun. *m*-Nitrobenzyl alcohol was used as a matrix.

^{1}H and ^{13}C NMR spectra were recorded at 303 K, in $CDCl_3$ solutions on a Varian INOVA 500 spectrometer, operated at 499.8, and 125.7 MHz for ^{1}H and ^{13}C, respectively. Chemical shifts were referenced against internal TMS (^{1}H spectra) or chloroform signal (^{13}C spectra – 77 ppm). The spectrometer was equipped with the 5 mm Nalorac Z-spec IDG inverse detection probe. 2D experiments including *g*-COSY, *g*-HSQC and *g*-HMBC were run by using the standard Varian software. The gradient selected ^{1}H - ^{13}C HSQC [6] and HMBC [7] NMR spectra were performed with an acquisition time of 0.2 s, a spectral width of 5000 Hz, 2048 data points in the ^{1}H dimension and 25000 Hz, 1024 increments in the ^{13}C dimension; 2 or 4 transients per t_1 increment, with a relaxation delay 1.5 s.

X-ray crystal structure determination: *Crystal data for (4)*. $C_{17}H_{26}O_{10}$, M_R = 390.38, orthorhombic, space group $P2_12_12_1$ (no. 19), a = 9.5287(6), b = 10.2916(10), c = 20.9500(10) Å. V = 2054.5(3) Å^3. Z = 4, D_{calc} = 1.262 g cm^{-3}, $F(000)$ = 832, T = 293 K, $\mu(CuK_\alpha)$ = 0.893 mm^{-1}, $\lambda(CuK_\alpha)$ = 1.54178 Å.

A colourless crystal of dimensions *ca*. 0.45 × 0.3 × 0.2 mm, cut from a larger one, was mounted on a glass fibre and placed on an Enraf-Nonius Mach-3 diffractometer. The unit cell parameters were obtained by a least-squares treatment of 25 centred reflections from the theta range of 23.18 and 43.21°. 3668 observed reflections [$I > 2\sigma(I)$], including Friedel opposites, were collected up to θ = 74.16° (R_{int} = 0.0127 for 3224 independent reflections). During the data collection, 7.5% declination of the intensities of 3 stan-

dard reflections was noticed. The data were corrected for Lorentz-polarization effects and the crystal deterioration. An experimental absorption correction based on ψ-scans was applied. The maximum and minimum transmission factors were 0.9904 and 0.9512, respectively. The structure was solved, using direct methods from SHELXS-97 program [8] and refined by a full-matrix least-squares on F^2 values applying SHELXL-97 software [9]. All the heavy atoms could be located from the first E-maps. After an anisotropic refinement of the partial model, subsequent difference density maps revealed all hydrogen atoms positions. In the final steps of refinement, the non-hydrogen atoms positions were refined together with their anisotropic displacement parameters, whereas hydrogen atoms positions were constrained to fulfil standard geometrical criteria for C–H bonds. The isotropic displacement parameters for methyl hydrogen atoms were taken as 1.5 of the isotropic equivalent of the respective carbon atoms and for other hydrogens as 1.2 of the respective values. During the refinement the isotropic extinction parameter was also varied. The final values of wR_2 and R_1 were 0.1600 and 0.0484, respectively. The weights used took the form $w = [\sigma^2(F_o^2) + (0.0988P)^2 + 0.5653P]^{-1}$, where $P = (F_o^2 + 2F_c^2)/3$. The obtained value of the Flack parameter [10] $x = 0.1(3)$ enabled us to ascribe the absolute configuration.

RESULTS AND DISCUSSION

Crystal structure analysis: We obtained crystals suitable for X-ray analysis only for **(4)**. Compound **(4)**, the isopropyl α-glucofuranoside tetraacetate, has molecular structure shown in Fig. 2. It has 5 asymmetric carbon atoms: C(1), C(2), C(3), C(4) and C(12). The respective configurations are S, R, S, R and R.

The atomic co-ordinates, anisotropic displacement parameters and torsion angles are collected in Tables 1, 2 and 3.

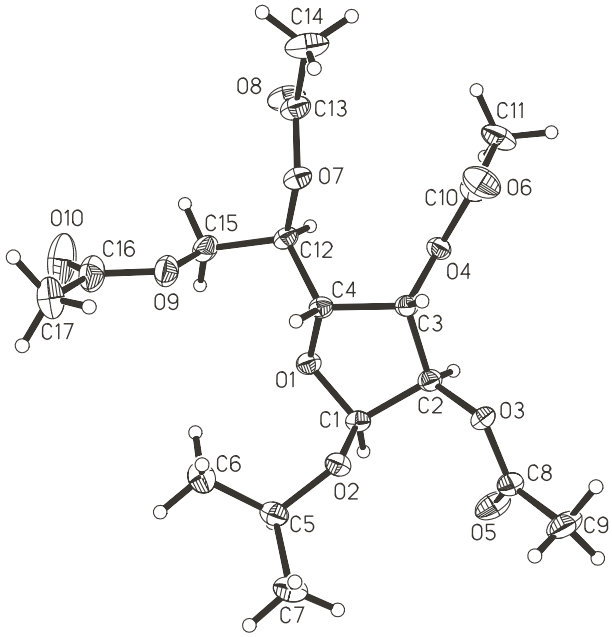

Figure 2. View of molecular geometry and a numbering scheme for α-glucoisopropylfuranoside tetraacetate. The non hydrogen atoms are shown as 30% probability ellipsoids.

Table 1. Atomic co-ordinates (x 10^4) and equivalent isotropic displacement parameters (Å^2 x 10^3) for **(4)**. U(eq) is defined as one third of the trace of the orthogonalized U_{ij} tensor.

	x	y	z	U(eq)
O(1)	3282(2)	6991(2)	10160(1)	47(1)
O(2)	1903(2)	7495(2)	11050(1)	48(1)
O(3)	1716(2)	9970(2)	10663(1)	51(1)
O(4)	2642(2)	9292(2)	9177(1)	47(1)
O(5)	3364(3)	10275(3)	11405(1)	82(1)
O(6)	580(3)	9881(3)	8745(1)	82(1)
O(7)	1504(2)	6801(2)	8645(1)	51(1)
O(8)	3003(3)	6593(3)	7822(1)	83(1)
O(9)	1682(3)	4547(2)	9422(1)	68(1)
O(10)	2649(4)	2627(4)	9279(3)	134(2)
C(1)	3033(3)	7868(3)	10670(1)	44(1)
C(2)	2651(3)	9122(3)	10323(1)	45(1)
C(3)	1939(3)	8685(3)	9706(1)	41(1)
C(4)	2179(3)	7209(3)	9710(1)	41(1)
C(5)	2171(4)	6396(3)	11465(2)	58(1)
C(6)	1708(7)	5167(4)	11158(2)	92(2)
C(7)	1400(6)	6686(5)	12078(2)	89(1)
C(8)	2199(4)	10476(4)	11215(2)	56(1)
C(9)	1100(5)	11260(5)	11544(2)	83(1)
C(10)	1825(4)	9844(3)	8718(2)	57(1)
C(11)	2716(5)	10374(5)	8195(2)	82(1)
C(12)	2643(3)	6584(3)	9086(1)	46(1)
C(13)	1829(4)	6762(4)	8016(2)	61(1)
C(14)	554(5)	6962(6)	7611(2)	92(2)
C(15)	2923(4)	5147(3)	9163(2)	60(1)
C(16)	1671(5)	3269(4)	9446(3)	81(1)
C(17)	339(6)	2739(5)	9709(3)	95(2)

Table 2. Anisotropic displacement parameters (Å^2 x 10^3) for **(4)**. The anisotropic displacement factor exponent takes the form: $-2\pi^2[h^2\, a^{*2}U^{11} + ... + 2\, h\, k\, a^*b^*U^{12}]$.

	U^{11}	U^{22}	U^{33}	U^{23}	U^{13}	U^{12}
O(1)	47(1)	52(1)	41(1)	–3(1)	–1(1)	7(1)
O(2)	50(1)	52(1)	41(1)	6(1)	2(1)	1(1)
O(3)	65(1)	46(1)	40(1)	–11(1)	–3(1)	4(1)
O(4)	53(1)	48(1)	39(1)	7(1)	3(1)	1(1)
O(5)	75(2)	105(2)	67(2)	–34(2)	–14(2)	–7(2)
O(6)	64(2)	104(2)	78(2)	28(2)	–14(1)	6(2)
O(7)	53(1)	62(1)	39(1)	–9(1)	2(1)	–1(1)
O(8)	76(2)	125(3)	48(1)	–13(2)	17(1)	–9(2)
O(9)	87(2)	45(1)	72(2)	–7(1)	15(2)	1(1)
O(10)	103(3)	62(2)	237(5)	–20(3)	6(3)	16(2)
C(1)	44(1)	52(2)	36(1)	0(1)	–2(1)	–3(1)
C(2)	49(1)	46(1)	38(1)	–3(1)	–1(1)	–6(1)
C(3)	44(1)	45(1)	35(1)	–1(1)	–2(1)	1(1)
C(4)	41(1)	47(2)	36(1)	–1(1)	5(1)	–1(1)
C(5)	65(2)	64(2)	45(2)	9(1)	–4(2)	0(2)
C(6)	140(4)	60(2)	76(3)	8(2)	14(3)	–10(3)
C(7)	126(4)	89(3)	51(2)	9(2)	21(2)	–5(3)
C(8)	71(2)	55(2)	43(2)	–5(1)	–8(2)	–4(2)
C(9)	97(3)	98(3)	54(2)	–34(2)	–15(2)	17(3)

Table 2 (continuation)

C(10)	69(2)	56(2)	45(2)	6(1)	–3(2)	5(2)
C(11)	94(3)	101(3)	51(2)	31(2)	4(2)	7(3)
C(12)	50(1)	51(2)	38(1)	–10(1)	5(1)	–1(1)
C(13)	67(2)	74(2)	43(2)	–10(2)	4(2)	–11(2)
C(14)	82(3)	142(5)	51(2)	–14(3)	–13(2)	–5(3)
C(15)	69(2)	53(2)	58(2)	–15(2)	5(2)	14(2)
C(16)	88(3)	49(2)	105(3)	–6(2)	–13(3)	9(2)
C(17)	108(3)	52(2)	124(4)	10(3)	3(3)	–3(2)

Table 3. Torsion angles [°] for **(4)**.

C(5)–O(2)–C(1)–O(1)	73.6(3)	C(2)–C(3)–C(4)–C(12)	–135.7(3)
C(5)–O(2)–C(1)–C(2)	–173.3(2)	C(1)–O(2)–C(5)–C(6)	–94.6(4)
C(4)–O(1)–C(1)–O(2)	73.4(3)	C(1)–O(2)–C(5)–C(7)	142.7(3)
C(4)–O(1)–C(1)–C(2)	–43.3(3)	C(2)–O(3)–C(8)–O(5)	2.7(5)
C(8)–O(3)–C(2)–C(1)	64.0(3)	C(2)–O(3)–C(8)–C(9)	–176.0(3)
C(8)–O(3)–C(2)–C(3)	–178.3(3)	C(3)–O(4)–C(10)–O(6)	2.4(5)
O(2)–C(1)–C(2)–O(3)	31.3(3)	C(3)–O(4)–C(10)–C(11)	–177.6(3)
O(1)–C(1)–C(2)–O(3)	150.7(2)	C(13)–O(7)–C(12)–C(15)	–81.6(3)
O(2)–C(1)–C(2)–C(3)	–88.4(3)	C(13)–O(7)–C(12)–C(4)	157.3(3)
O(1)–C(1)–C(2)–C(3)	31.0(3)	O(1)–C(4)–C(12)–O(7)	179.1(2)
C(10)–O(4)–C(3)–C(2)	–133.8(3)	C(3)–C(4)–C(12)–O(7)	–63.0(3)
C(10)–O(4)–C(3)–C(4)	113.8(3)	O(1)–C(4)–C(12)–C(15)	58.8(3)
O(3)–C(2)–C(3)–O(4)	109.8(2)	C(3)–C(4)–C(12)–C(15)	176.7(3)
C(1)–C(2)–C(3)–O(4)	–126.3(2)	C(12)–O(7)–C(13)–O(8)	–2.0(5)
O(3)–C(2)–C(3)–C(4)	–132.1(2)	C(12)–O(7)–C(13)–C(14)	178.3(3)
C(1)–C(2)–C(3)–C(4)	–8.2(3)	C(16)–O(9)–C(15)–C(12)	171.7(3)
C(1)–O(1)–C(4)–C(12)	163.9(2)	O(7)–C(12)–C(15)–O(9)	–61.7(3)
C(1)–O(1)–C(4)–C(3)	38.7(3)	C(4)–C(12)–C(15)–O(9)	55.5(4)
O(4)–C(3)–C(4)–O(1)	98.8(2)	C(15)–O(9)–C(16)–O(10)	2.0(7)
C(2)–C(3)–C(4)–O(1)	–17.2(3)	C(15)–O(9)–C(16)–C(17)	–178.9(4)
O(4)–C(3)–C(4)–C(12)	–19.7(3)		

The four acetoxy groups show some degree of enhanced thermal motion, which is visible in an elongation of thermal ellipsoids for the carbonyl oxygen and the methyl carbon atoms in directions perpendicular to the planes of the given groups. A similar vibrational motion is also visible for the isopropyl group. In the crystal structure only weak C–H···O hydrogen bonds are discernible. Their geometries are summarized in Table 4.

Table 4. Hydrogen bonds for **(4)** [Å and °].

D–H···A	d(D–H)	d(H···A)	d(D···A)	<(DHA)
C(9)–H(9B)···O(8)#1	0.96	2.65	3.576(5)	161.1
C(1)–H(1)···O(7)#2	0.98	2.66	3.621(4)	165.8

Symmetry transformations used to generate equivalent atoms:
#1 –x + 1/2, –y + 2, z + 1/2; #2 x + 1/2, –y + 3/2, –z + 2.

All molecular distances and angles have acceptable values.

Structure of isopropylglucofuranosides as studied by ^{1}H and ^{13}C NMR: The ^{1}H NMR data of isopropyl glucosides refer to β-isopropyl glucopyranoside [11]. Full proton NMR data of the α anomer are not reported. Lemieux [12] stated that a reaction of 1,2 acylspiroorthoesters of 3,4,6 tri-O-acetyl α-glucopyranose with propanol-2 catalyzed by tin tetrachloride produces a mixture of α- and β-isopropylglucopyranosides in a 5:4 ratio, as determined by their anomeric doublets: H1α at 5.01 and H1β at 4.52. The isolation of products was not performed. The ^{13}C NMR spectra of both isopropylglucopyranosides are known [13]. To our best knowledge, both α- and β-isopropylglucofuranosides were not described in literature. Synthesis and isolation of butyl glucopyranosides and furanosides was described [3a], but full assignments of ^{1}H chemical shifts (except for anomeric proton H1) and coupling constants of furanosides were not done. Besides measuring spectra for **(1)** and **(2)**, in order to avoid complications arising from measuring of polyhydroxy compounds, we measured NMR spectra of peracetylated derivatives **(3)** and **(4)**. Their spectra in $CDCl_3$ were stable. Full proton assignments were done on the basis of 2D COSY and *J*-proton-proton coupling pattern. The results are shown in Tables 5 and 6. Atom numbering is shown in Fig. 3.

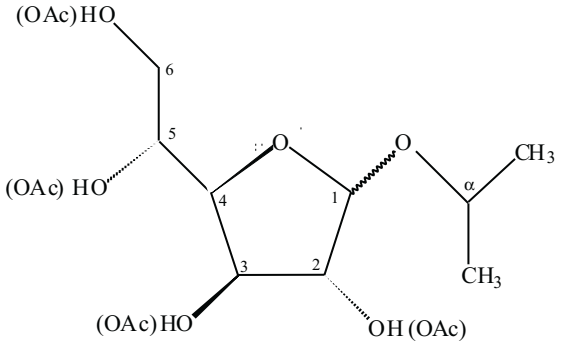

Figure 3. Atom numbering scheme for α- and β-isopropylglucofuranosides and their tetraacetates.

Table 5. ^{1}H chemical shifts (δ) of studied glucofuroanosides in $CDCl_3$[a)].

	H1	H2	H3	H4	H5	H6a	H6b	Hα	Me-a	Me-b
(1)	5.04	4.14	4.22	4.20	3.93	3.86	3.77	3.91	1.19	1.16
(2)	5.22	4.06	4.32	4.02	3.91	3.82	3.64	3.96	1.24	1.18
(3)	5.09	4.96	5.34	4.46	5.28	4.62	4.17	3.90	1.22	1.16
(4)	5.38	4.87	5.55	4.41	5.23	4.53	4.14	3.83	1.20	1.10

[a)] 0.05 Mdm^{-3}.

Table 6. The proton-proton coupling constants of studied glucofuroanosides in $CDCl_3$.

	$^{3}J_{H1-H2}$	$^{3}J_{H2-H3}$	$^{3}J_{H3-H4}$	$^{3}J_{H4-H5}$	$^{3}J_{H5-H6a}$	$^{3}J_{H5-H6b}$	$^{3}J_{H6a-H6b}$
(1)*	–	–	–	–	–	–	–
(2)	4.3	3.3	4.6	7.9	2.8	6.7	11.6
(3)	1.4	1.0	5.1	9.4	2.4	4.9	12.3
(4)	4.7	2.8	5.0	9.0	2.4	5.3	12.3

*Data of compound **(1)** not obtained due to signal broadening.

The ^{13}C chemical shifts were determined unambiguously through 2D HSQC proton-carbon connectivities and are shown in Table 7.

Table 7. The ^{13}C chemical shifts (δ) of studied glucofuroanosides in $CDCl_3$.

	C1	C2	C3	C4	C5	C6	Cα	Me-a	Me-b
(1)	106.0	80.0	76.2	81.0	70.6	64.1	70.3	23.5	21.4
(2)	100.1	77.8	76.5	78.0	70.6	64.2	71.5	23.4	22.0
(3)	104.4	80.8	73.6	77.9	68.9	63.3	70.2	23.2	21.3
(4)	99.4	78.7	74.6	73.8	68.1	63.0	72.0	23.3	21.9
(1) (D_2O)	107.2	80.9	75.8	81.4	70.5	64.3	72.4	22.9	21.5

For compounds **(3)** and **(4)**, the HMBC technique was used as a final and unequivocal tool to prove a five-member glucoside ring structure (cross peaks H1 – C4 and H4 – C1) and a substitution of propanol-2 in an anomeric position (cross peaks H1 – Cα, Hα – C1) (Fig. 4).

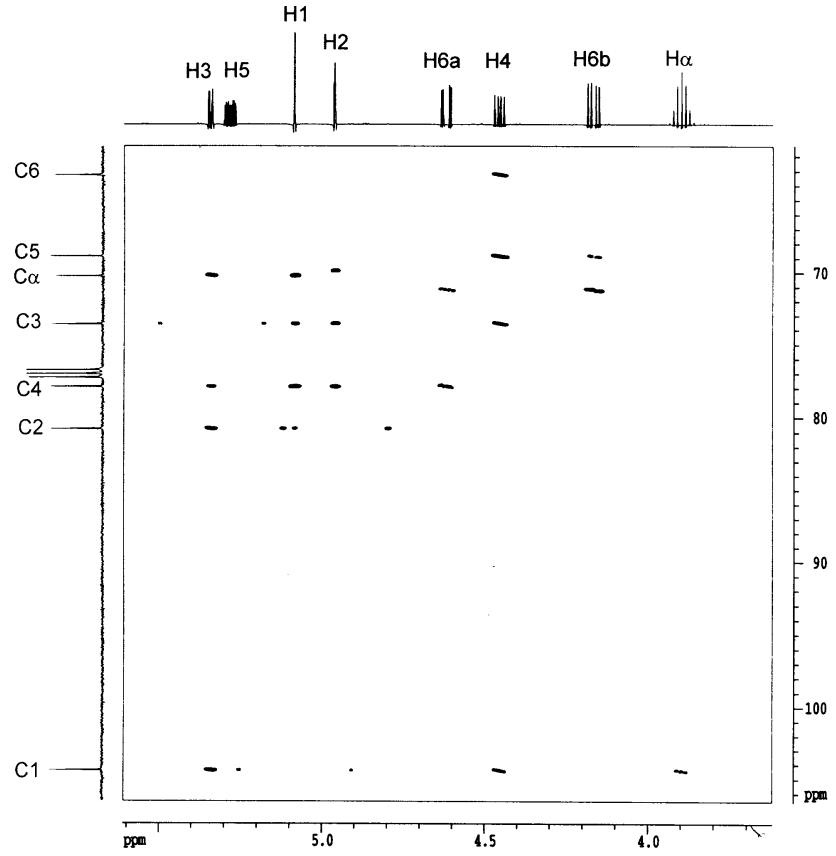

Figure 4. Partial contour plot of the ^{1}H–^{13}C *g*-HMBC spectrum of α-isopropylglucofuranoside tetraacetate.

We have performed the calculations of geometry in solution of compounds **(3)** and **(4)**, using PSEUROT v 6.3 program [14]. This program was designed to model pseudorotation parameters P and φ on the basis of NMR derived vicinal coupling constants and a generalized Karplus equation. According to a pseudorotational concept, a conformation of a puckered five-membered ring can be described by two parameters: the phase angle of pseudorotation (P), which defines the part of ring, which is mostly puckered, and the puckering amplitude (φ), which indicates the extent of puckering. These two parameters define all five endocyclic torsion angles. The software calculates the best fit of conformational parameters for two conformers, assuming that a two-state equilibrium in solution is present, and the coupling constants represent time-averaged values of couplings of individual conformers. However, for compounds **(3)** and **(4)** we have observed a strong preference for only one conformer, the rewarding good fit was obtained, when there was less than 5% of the minor conformer. The calculated values of conformational parameters, together with calculated vicinal coupling constants and RMS values of calculated *vs*. experimental coupling for a major conformer are given in Table 8.

Table 8. Calculated torsion angles, coupling constants, and puckering parameters for solution conformation of compounds **(3)** and **(4)**.

		H1-H2	H2-H3	H3-H4	P	Φ	RMS
(3)	φ	78.9	–90.9	–7.7	–50°	41°	0.055
	^3J	1.46	1.07	5.12			
(4)	φ	30.1 (32.4)[a]	–134.1 (–132.1)[a]	–8.3 (–19.3)[a]	–119°	26°	0.12
	^3J	4.53	2.73	5.07			

[a]In parentheses are given values of torsion angles for X-ray derived structure of compound **(4)**.

A comparison of calculated and experimental values of the vicinal constants led us to the conclusion, that compound **(4)** has an α-furanose configuration. The NMR data in solution for compound **(4)** are consistent with the X-ray structure shown in Fig. 2. A calculated solution conformation of compound **(4)** appeared to be in an excellent agreement with the crystal structure, indicating that there are no major conformational changes in solution.

Unfortunately, the crystals of **(3)** for the X-ray analysis could not be obtained. However, the comparison of NMR data in Tables 5–7 for **(3)** and **(4)** leads to the conclusion that the major differences are around anomeric site. This suggests, that compound **(3)** is a β-furanoside. This is directly confirmed by the C^1 chemical shift difference of 5 ppm and a small value of ^3J(H1, H2) with respect to the respective parameter for **(4)**. Furthermore, a modelling of a vicinal coupling constant for **(3)**, using the PSEUROT v 6.3 program, shows that a good fit of calculated and experimental values is obtained

only for a model having a β-furanose configuration with an original D-glucose stereochemistry for other ring carbon atoms.

Hypothesis of the reaction mechanisms: Reactions were performed according to the scheme:

$$\text{Glc} + i\text{-PrOH} \xrightarrow[\text{boiling } i\text{-PrOH}]{\text{suspended vanadia}} \text{heterogeneous reaction mixture} \longrightarrow \quad (1)$$

$$\longrightarrow \text{evaporation of } i\text{-PrOH, soxhlet extraction} \longrightarrow \text{crude product} \quad (2)$$

Mechanism of glycosidation of D-glucose with n-butanol catalyzed by dealuminated H-Y fujasites was discussed by Chapat *et al*. [4b]. The first step is a protonation of D-glucose ring oxygen, so Brönsted acidity of a catalyst is crucial. Protonation is followed by a simultaneous dehydration, reaction with ROH and the C1–O bond cleavage, so eventually the sort of noncyclic carbonium ion is formed. Internal rotations for this ion are possible and a furanoside ring can be closed. It is widely accepted, that glycosidation with alcohols is a proton catalyzed process [15]. We observed the glycosidation with vanadium oxide, which has no Brönsted acid sites [16]. However, V_2O_5 can cause water dissociation: OH^- combines with vanadium by an oxygen end; proton connects vanadyl oxygen and a four member ring is formed. A proton originating from water forms a hydrogen bond between two oxygens [16]. Such a process is likely with *i*-PrOH what is shown in Fig. 5.

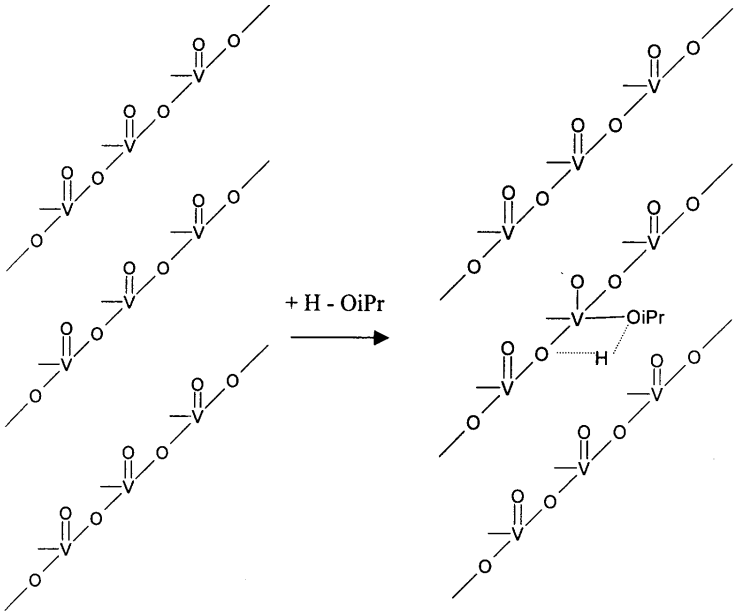

Figure 5. Scheme of dissociation of propanol-2 on vanadia surface, analogous to water dissociation, (Busca [16]).

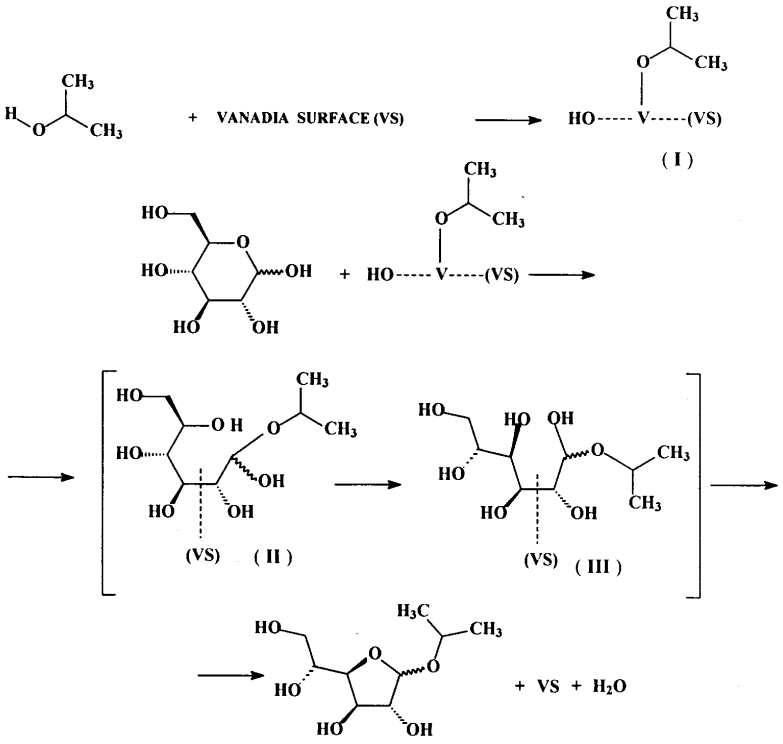

Figure 6. Hypothesis of the selective glycosidation of D-glucose by propanol-2 promoted by vanadia.

This is a first step of our mechanistic hypothesis, shown in Fig. 6 , where intermediate **I** is formed.

The second step consists of a synchronic protonation of D-glucose ring oxygen, cleavage of C1–O bond and an addition of RO^{-} to C1 carbon. The adsorbed open chain intermediate (**II**) is formed. It can rearrange further and an adsorbed precursor of a furanoside ring is formed (**III**). The most probable way of connecting intermediates (**II**) and (**III**) with surface is by –OH groups. In Fig. 6 it is symbolized by a broken line. The precise nature of this connection needs an additional study. Formation of (**III**) is a crucial step for the observed selectivity. Such precursor collapses to final α- and β-isopropyl glucofuranosides, but not pyranosides. Neither α- nor β-isopropylglucopyranoside is observed in our reaction. In all reactions of butanol with glucopyranose catalyzed by dealuminated HY fujasites [4b], the formation of all four isomers of butylglucosides was always detected, among them α-butylpyranoside was the thermodynamically most stable isomer [4b]. To understand better the selectivity in this case, one needs a further study of a surface reaction mechanism.

Acknowledgments

Mrs Elżbieta Świech and Mrs Dorota Łuniewska are grateful acknowledged for technical assistance.

REFERENCES

1. Hughes F.A. and Lew B.W., *J. Am. Oil Chem. Soc*., **47**, 162 (1970).
2. a) Hensen H., Busch P., Krächter H.U. and Hatesman, *Tensid. Surf. Det.,* **30**, 116 (1993); b) Mentech J., Beck R. and Burzio F., Carbohydrates as Organic Raw Materials, Ed. G. Descotes, VCH Publ. Weinheim/NY, p. 185 (1993).
3. a) Straathof A.J.J., Romein J., Van Rantwijk F., Kieboom F. and Van Bekkum H., *Starch/Stärke*,**39**, 362 (1987); b) Straathof A.J.J., Van Bekkum H. and Kieboom A.P.G., *Starch/Stärke*, **40**, 229 (1988).
4. a) Corma A., Iborra S., Miquel S. and Primo J.J., *J. Catal.,* **161**, 713 (1966); b) Chapat J-F., Finiels A., Joffre J. and Moreau C., *J. Catal*., **185**, 445 (1999).
5. Brochette S., Descotes G., Bouchu A., Queneau Y., Monnier N. and Petrier C., *J. Mol. Catal. A Chem.*, **123**, 123 (1997).
6. Summers M.F.J., Marzili L.G. and Bax A., *J. Am. Chem. Soc*., **108**, 4285 (1986).
7. Bax A. and Summers M.F.J., *J. Am. Chem. Soc*., **108**, 2093 (1986).
8. Sheldrick G.M., *Acta Cryst*., **A46**, 467 (1990).
9. Sheldrick G.M. SHELXL-97, Program for Crystal Structure Refinement, University of Göttingen, Germany.
10. Flack H.D., *Acta Cryst*., **A39**, 876 (1983).
11. Du X.-M., Yoskikawa T. and Yukihiro S., *Phytochem*., **49**, 1925 (1998).
12. Lemieux R.V. and Hindsgaul O., *Carbohydr. Res*., **82**, 195 (1980).
13. Seo S., Tomita Y., Tori K. and Yoshimura Y., *J. Am. Chem. Soc*., **100**, 3331 (1978).
14. Van Wijk J., Haasnoot C.A.G., de Leeuw F.A.A.M., Huckriede B.D., Hoekzema A.W. and Altona C., PSEUROT 6.3, Leiden Institute of Chemistry, Leiden University, The Netherlands (1999).
15. Furniss B., Hannaford A.J., Smith P.W.G. and Tatchell A.R., Vogel's textbook of practical organic Chemistry, Vth Edition, Longmanscientific & Technical, 1989, p. 644.
16. Busca G., Ramis G. and Lorenzelli V., *J. Mol. Catal*., **50**, 231 (1989).